Supplementary Information for

Poleward Migration as Global Warming's Possible Self-Regulator to Restrain Future Western North Pacific Tropical Cyclone's Intensification

I-I Lin[1*], Suzana J. Camargo[2], Chun-Chi Lien[1], Chun-An Shi[1], & James P. Kossin[3]

[1]Department of Atmospheric Sciences, National Taiwan University, Taipei, Taiwan

[2]Lamont-Doherty Earth Observatory, Columbia University, Palisades, NY, USA

[3]The Climate Service, Durham, NC, & University of Wisconsin-Madison, USA

*Corresponding author: I-I Lin, Department of Atmospheric Sciences, National Taiwan University, Taipei, Taiwan. Email: iilin@ntu.edu.tw

Contents of this file:

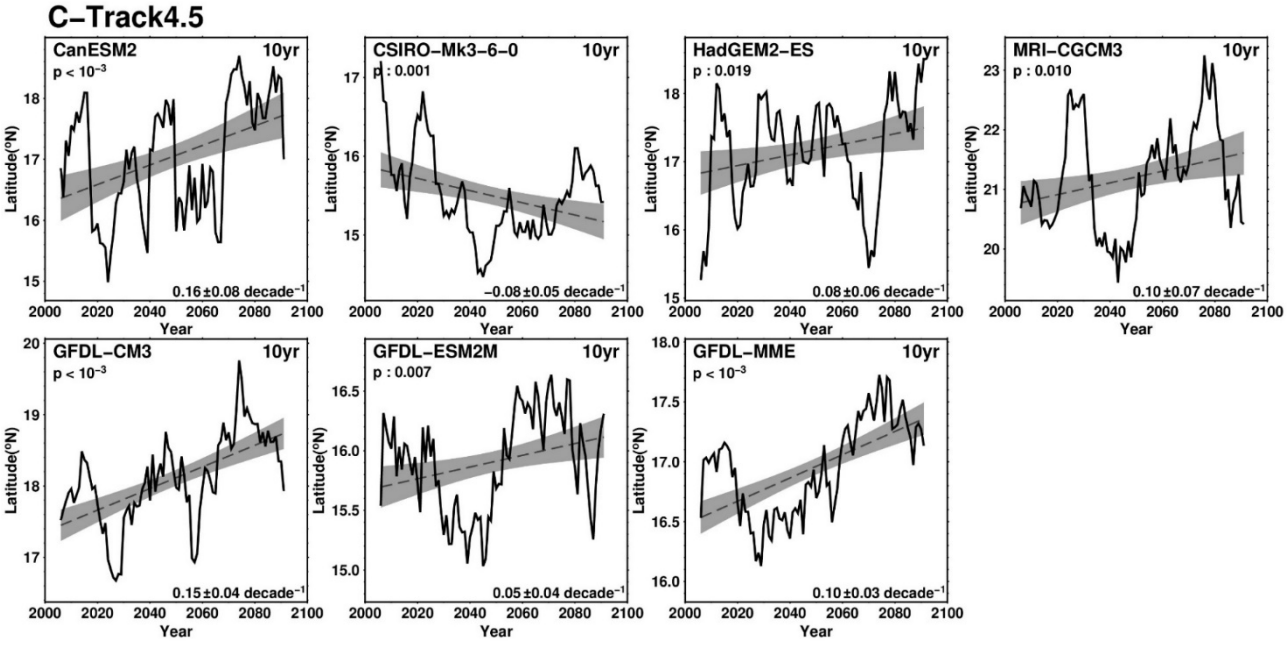

Supplementary Figure 1: Latitude time series for the 6 C-Track-4.5 individual model members. Time series for GFDL-MME (the 7th figure) is also depicted, based on the average of GFDL-CM3 and GFDL-ESM2M.

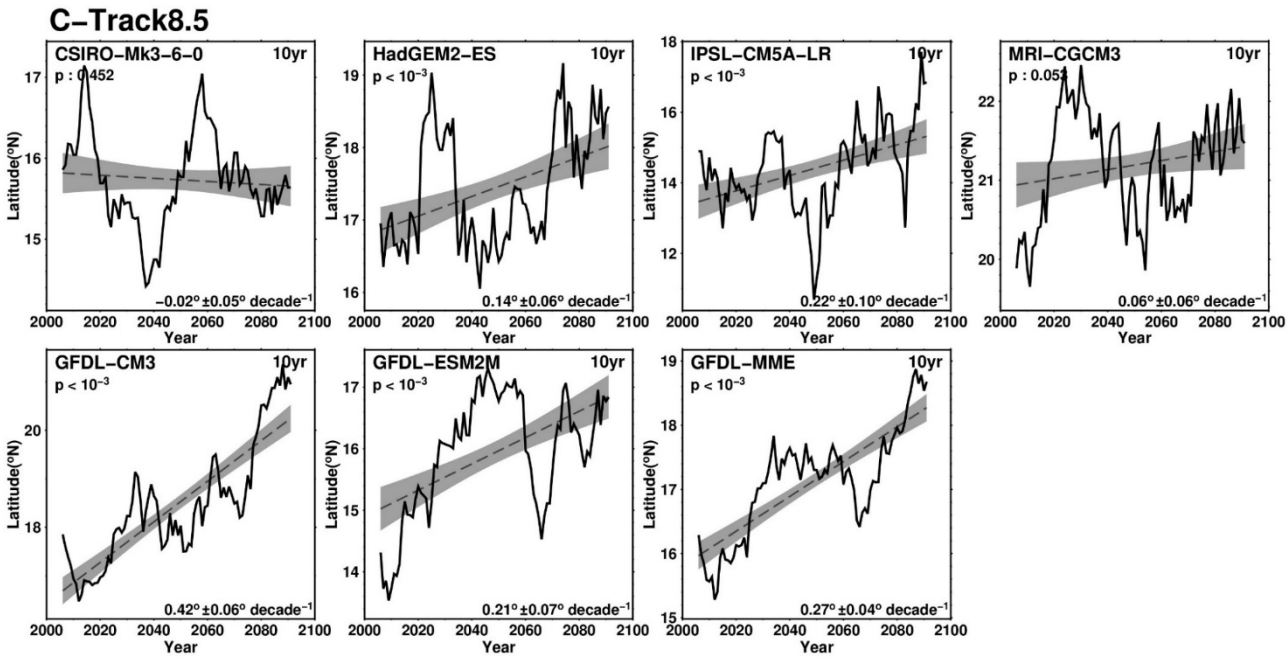

Supplementary Figure 2: Latitude time series for the 6 C-Track-8.5 individual model members. Time series for GFDL-MME (the 7th figure) is also depicted, based on the average of GFDL-CM3 and GFDL-ESM2M.

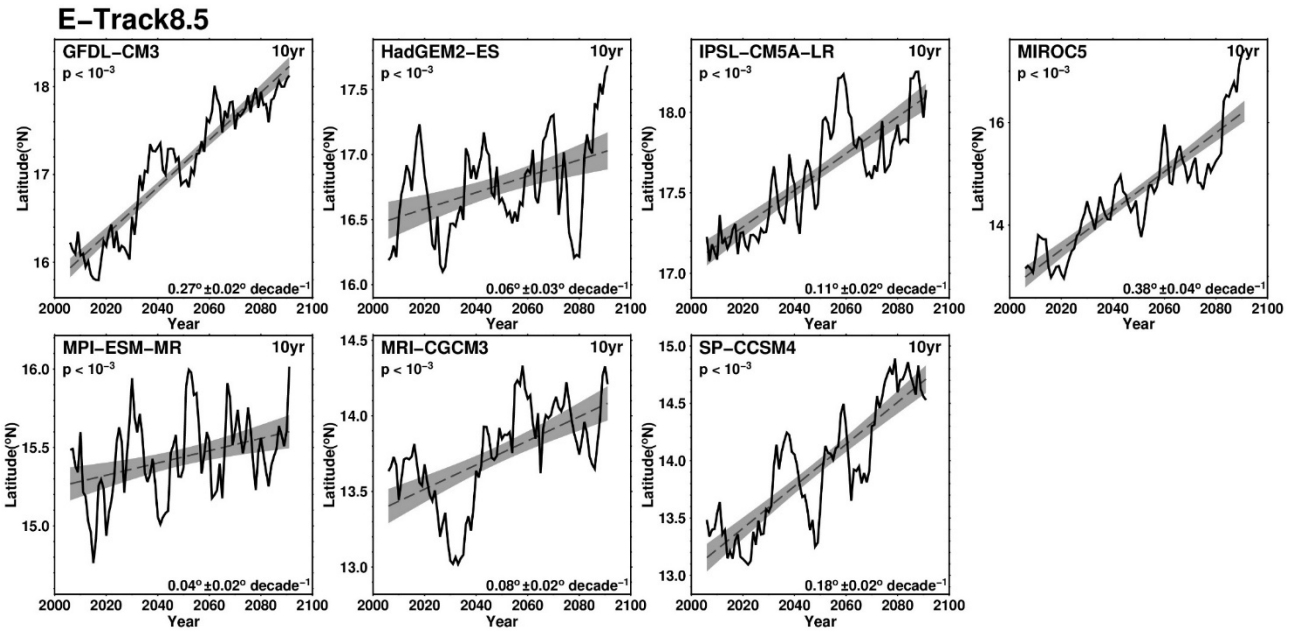

Supplementary Figure 3: Latitude time series for the 7 E-Track-8.5 individual model members.

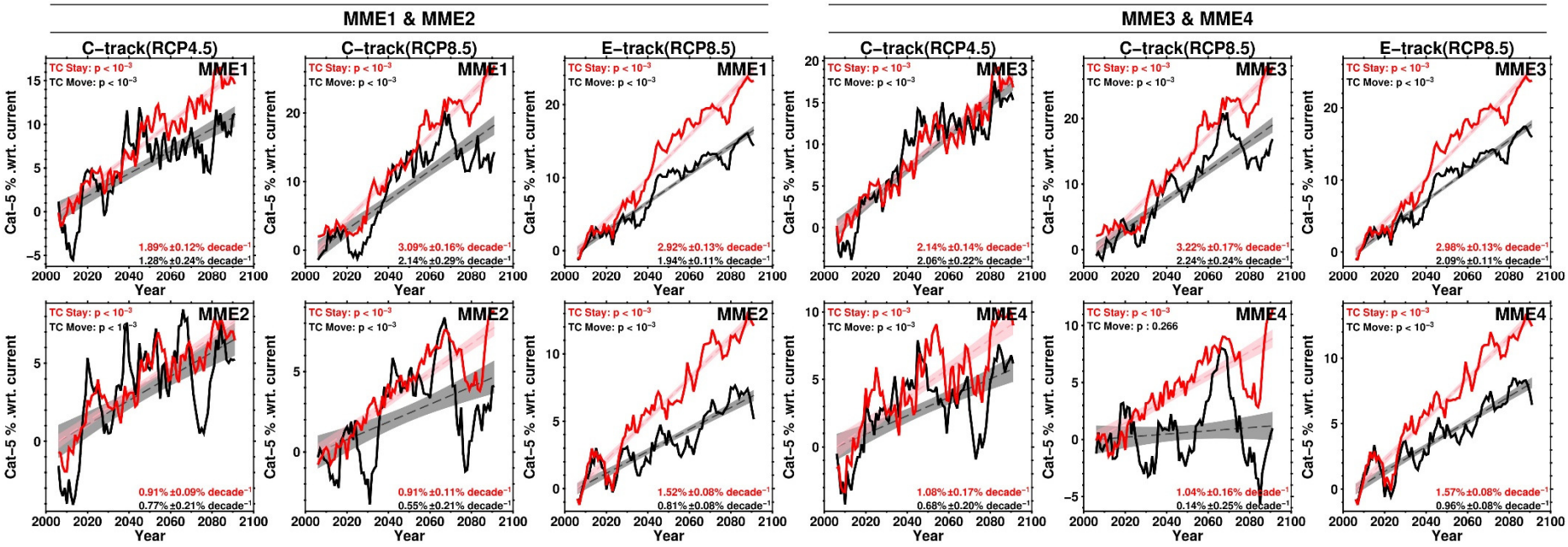

Supplementary Figure 4: Time series of the proportion of Category-5 PI, comparing with and without poleward migration situation (i.e., TC Move vs. TC Stay). Results for all 12 MMEs (3 TC track groups and 4 MMEs each) are shown. Left (Right) panels are the results of MME1 and MME2 (MME3 and MME4).

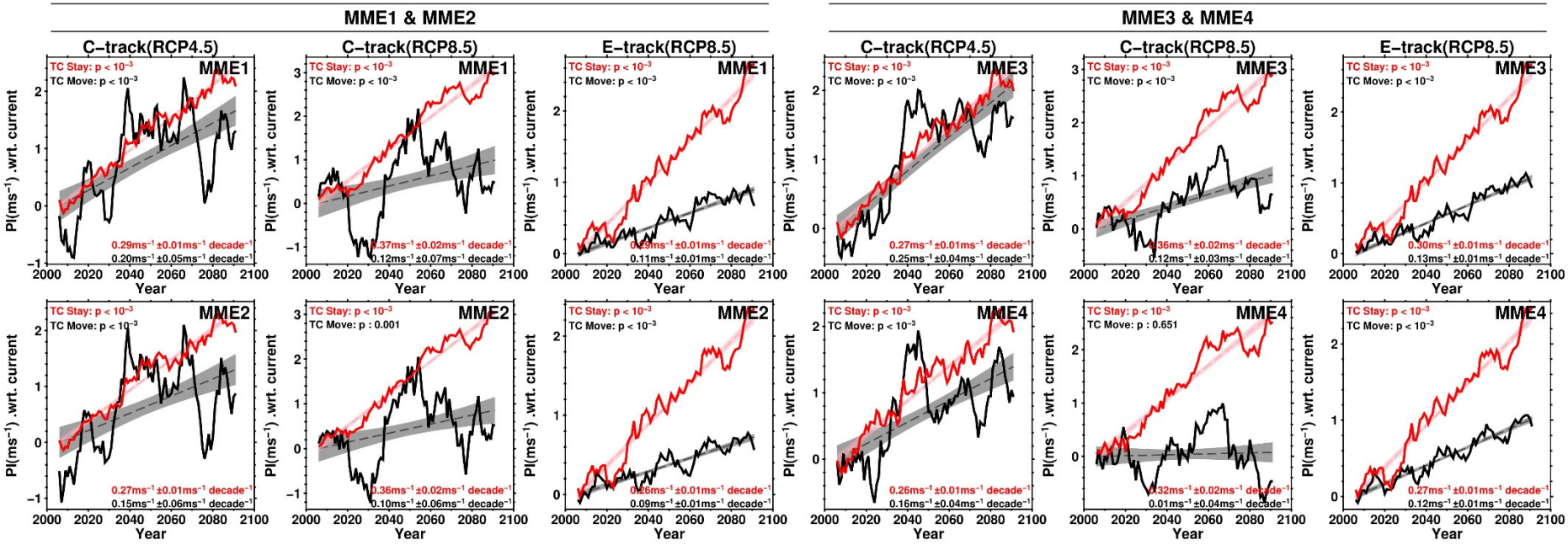

Supplementary Figure 5: Time series of the average PI, comparing with and without poleward migration situation (i.e., TC Move vs. TC Stay). Results for all 12 MMEs (3 TC track groups and 4 MMEs each) are shown. Left (Right) panels are the results of MME1 and MME2 (MME3 and MME4).

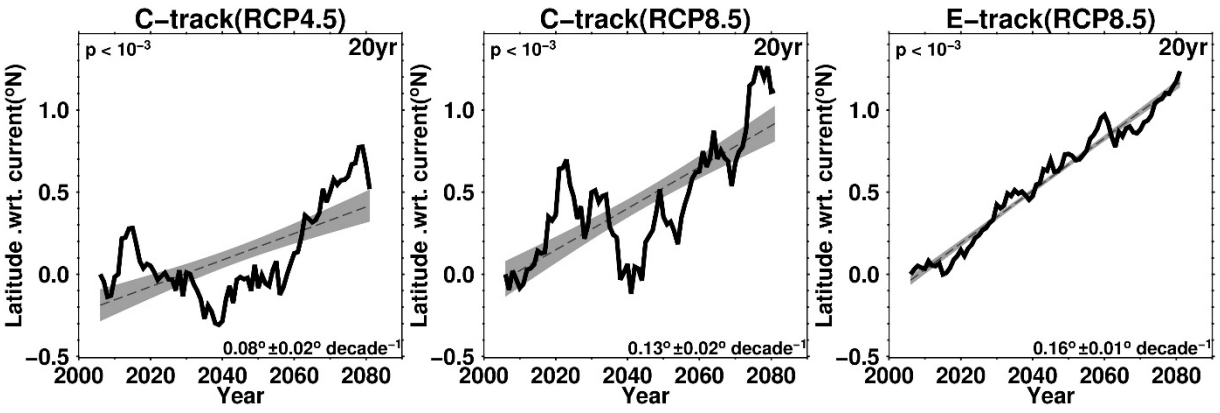

Supplementary Figure 6: MME-averaged latitude time series of the 3 TC track groups for the 20-year low-pass filter result, with trends and p-values. 95% confidence trend bounds are shaded.

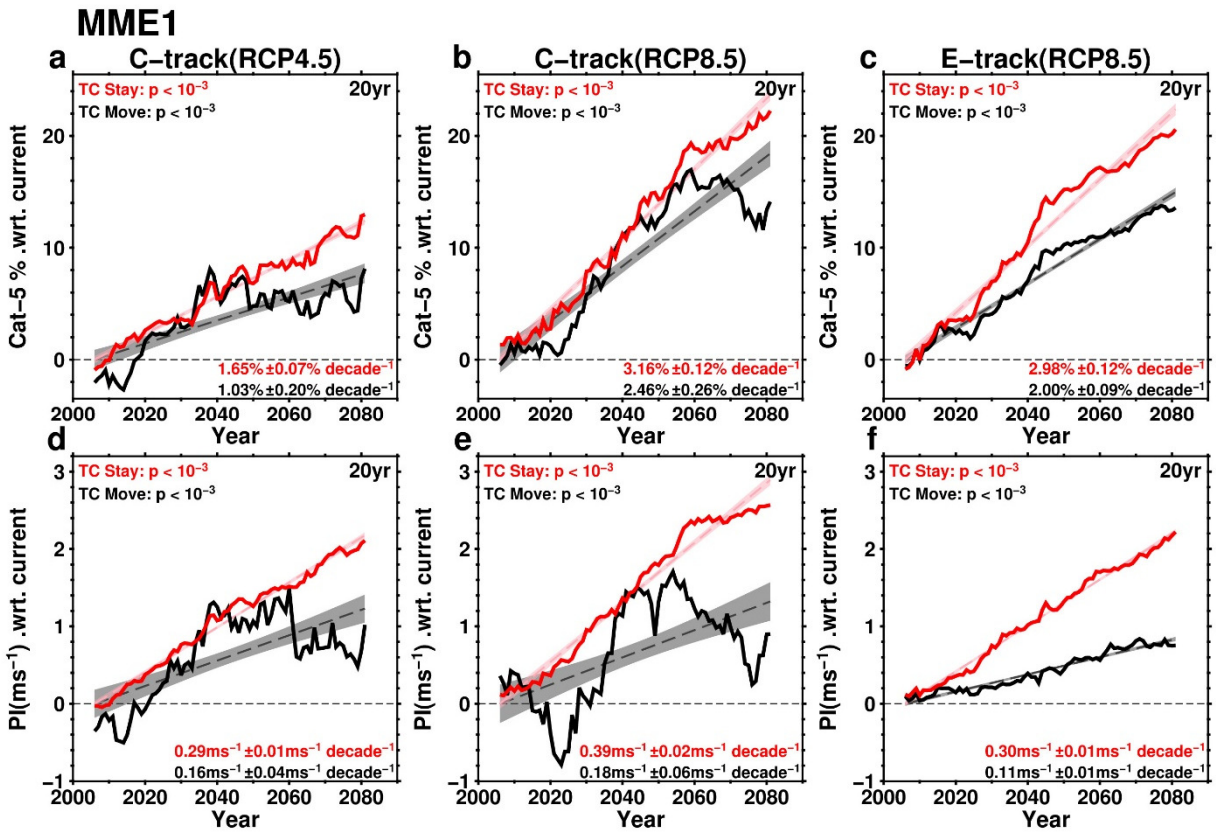

Supplementary Figure 7: Top (a, b, c): Proportion of Category-5 PI time series of the 3 track groups for the 20-year low-pass filter result, with trends and p-values, based on MME1. **Bottom (d, e, f):** As top, but for averaged PI. The regression lines are aligned at the zero point for trend comparison.

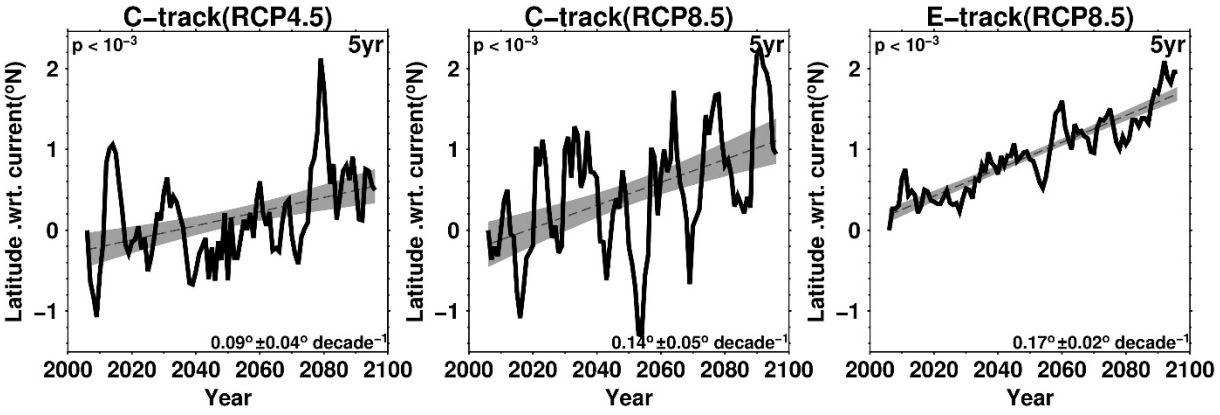

Supplementary Figure 8: MME-averaged latitude time series of the 3 TC track groups for the 5-year low-pass filter result, with trends and p-values. 95% confidence trend bounds are shaded.

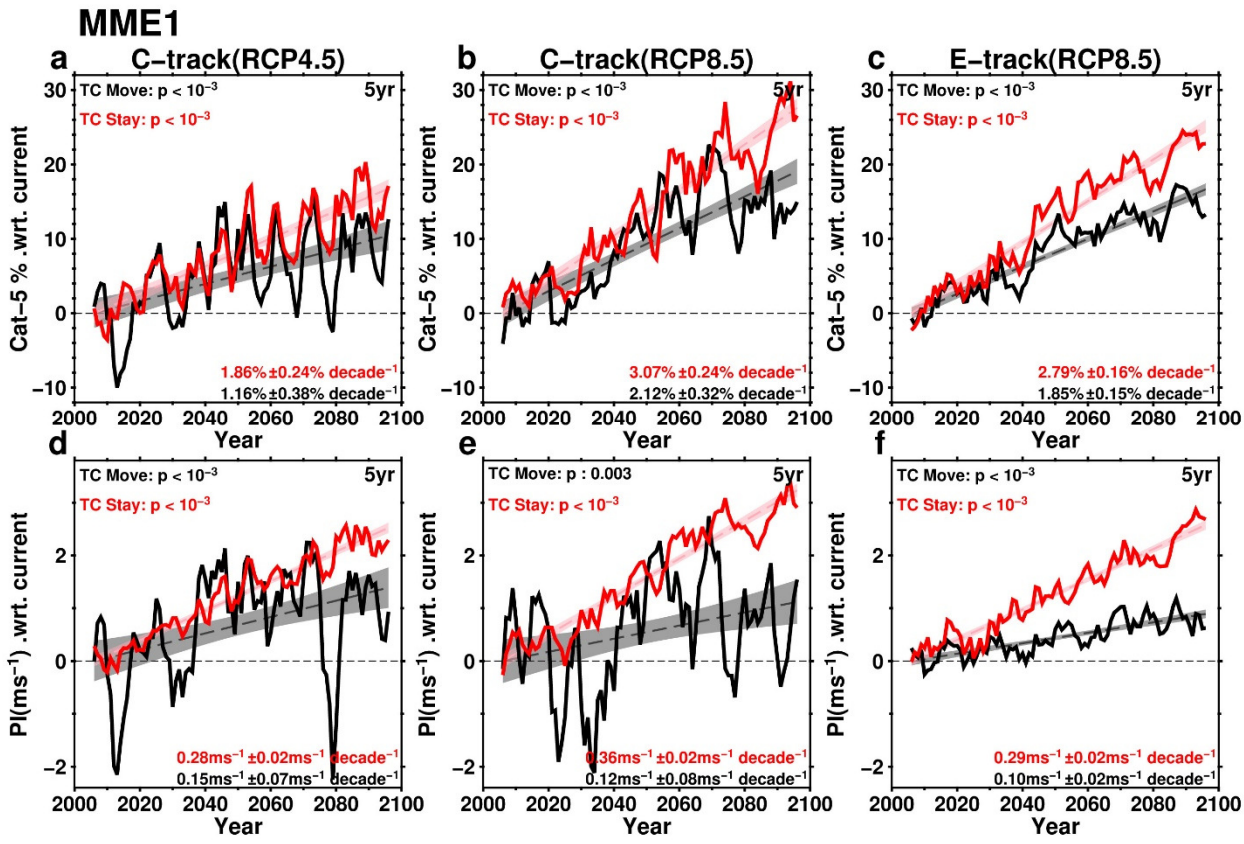

Supplementary Figure 9: Top (a, b, c): Proportion of Category-5 PI time series of the 3 track groups for the 5-year low-pass filter result, with trends and p-values, based on MME1. **Bottom (d, e, f):** As top, but for averaged PI. The regression lines are aligned at the zero point for trend comparison.

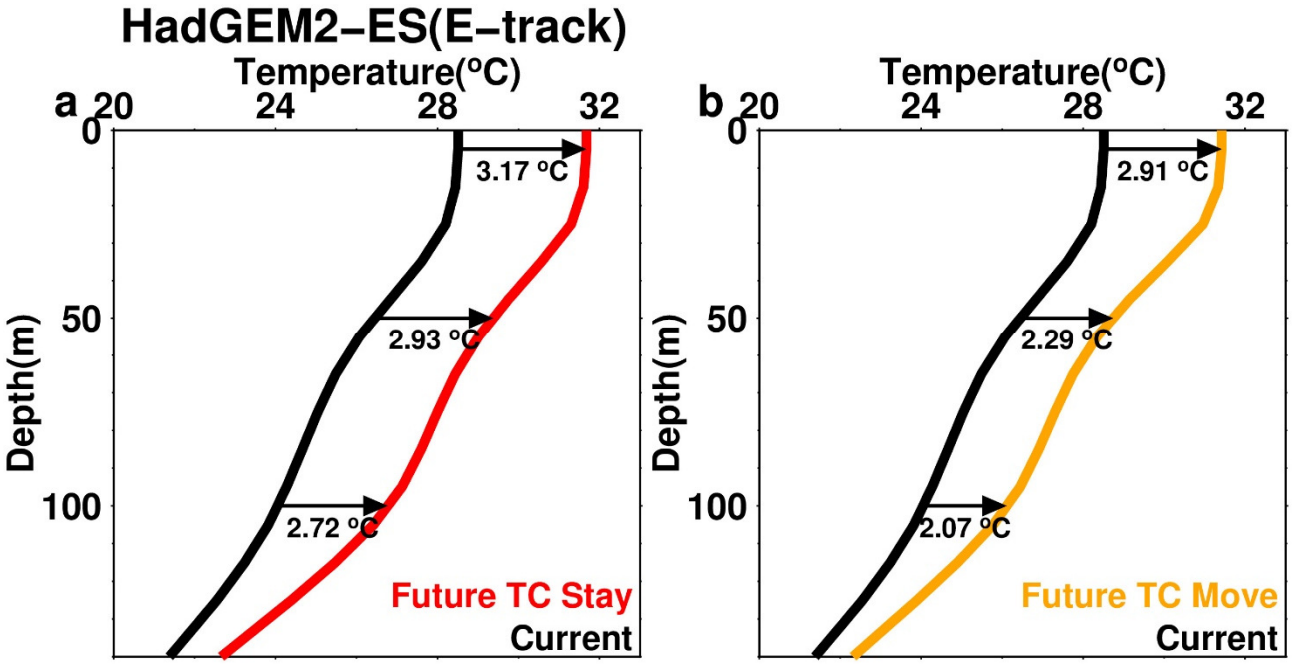

(c) E-Track-8.5/ HADGEMS2-ES	Current	Future TC Stay	Future TC Move
Pre-TC SST (˚C)	28.51	31.68	31.42
SST cooling (˚C)	-0.21	-0.31	-0.32
PI change w.r.t current (ms^{-1})	-	2.96	1.55
OCPI change w.r.t current (ms^{-1})	-	1.69	0.11

- PI: Difference between Future TC-Move and Future TC Stay is -1.41 ms^{-1} (i.e., 1.55 - 2.96). This difference is contributed by the 4 PI inputs.
- OCPI: Difference between Future TC-Move and Future TC Stay is -1.58 ms^{-1} (i.e., 0.11-1.69). This difference is contributed by the 5 OCPI inputs.
- The difference between -1.41 ms^{-1} and -1.58 ms^{-1}, i.e. -0.17 ms^{-1} is the contribution from ocean cooling (stratification) input. Thus ocean stratification contributes to ~ 11% in the total contribution from all 5 inputs (-0.17/-1.58).

Supplementary Figure 10: (a) Initial ocean thermal profiles for Current (black) and TC_Stay future scenario (red). (b) Initial ocean thermal profile for Current (black) and TC_Move future scenario (yellow). (c) Results of the ocean cooling effect, PI, and OCPI (Ocean Coupling Potential Intensity).

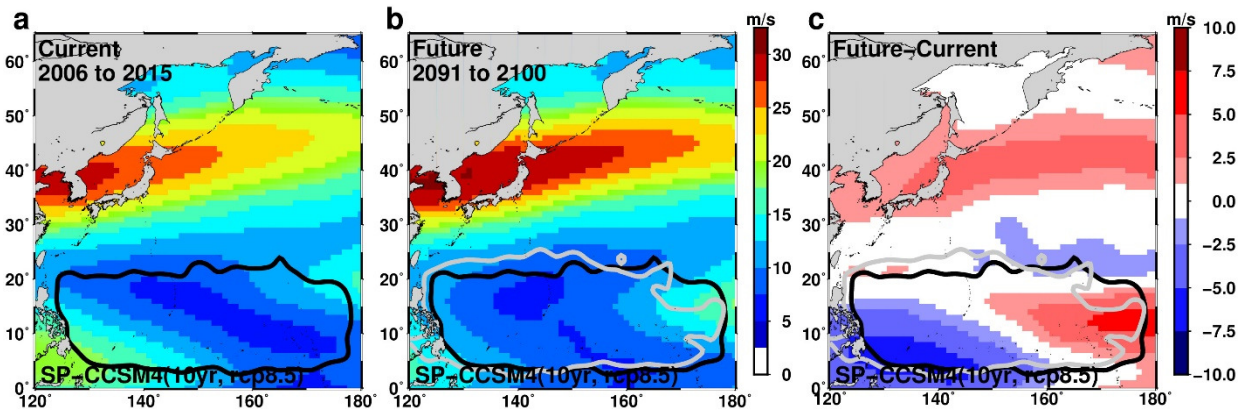

Supplementary Figure 11: Vertical wind shear (VWS) map with TC location contour overlaid for the E-Track-8.5 SP-CCSM4 model. TC location contour is based on the locations of the intensification track (IT) points. These points (2hrly-interval) are first interpolated to 3° by 3° grid before contouring, 80% of points are enclosed. The black contour in (a) is for the current TC location. For (b), 2 contours are shown, the black contour is the same as in (a), i.e. for the TC_Stay future scenario. The grey contour is for the TC_Move future scenario. In (c), the 2 contours are the same as in (b), but over the VWS anomaly between future (2091-2100) and current (2006-2015).

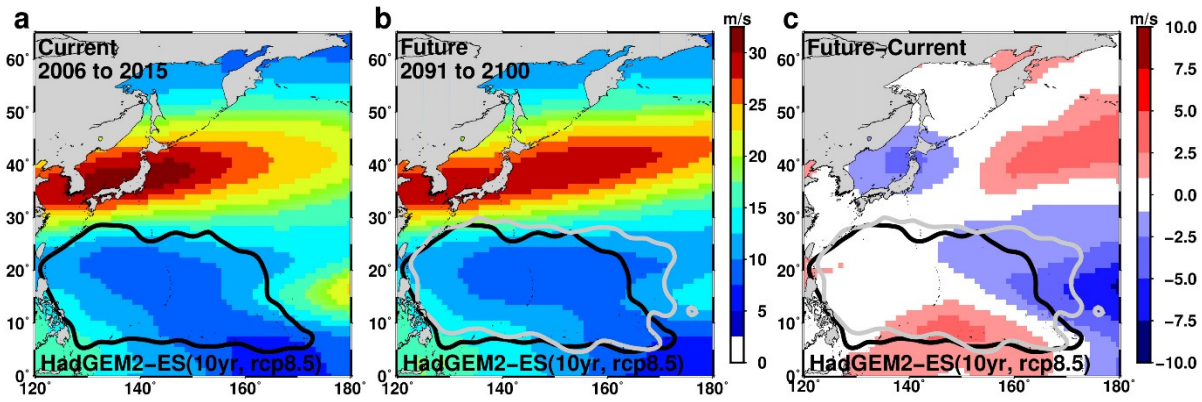

Supplementary Figure 12: Vertical wind shear (VWS) map with TC location contour overlaid for the E-Track-8.5 HADGEMS2-ES model. TC location contour is based on the locations of the intensification track (IT) points. These points (2hrly-interval) are first interpolated to 3° by 3° grid before contouring, 80% of points are enclosed. The black contour in (a) is for the current TC location. For (b), 2 contours are shown, the black contour is the same as in (a), i.e. for the TC_Stay future scenario. The grey contour is for the TC_Move future scenario. In (c), the 2 contours are the same as in (b), but over the VWS anomaly between future (2091-2100) and current (2006-2015).

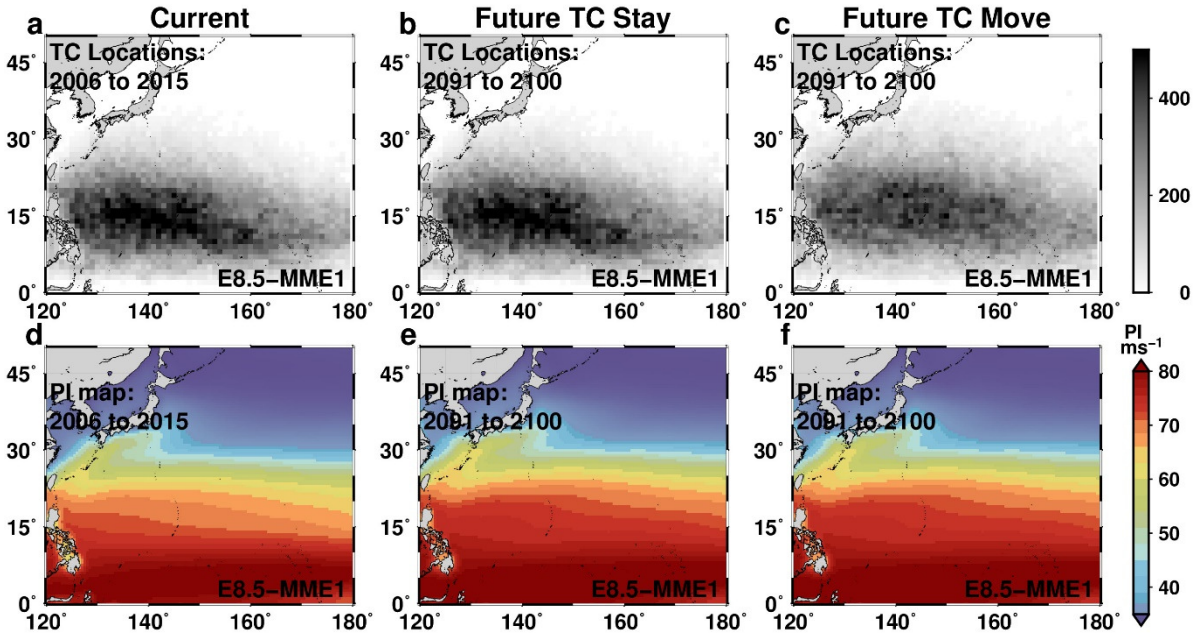

Supplementary Figure 13: Top panel: TC IT point comparison between current (a) and the 2 future scenarios (b, c), based on E-Track-8.5 MME1. Bottom panel: as top, but for PI map comparison.

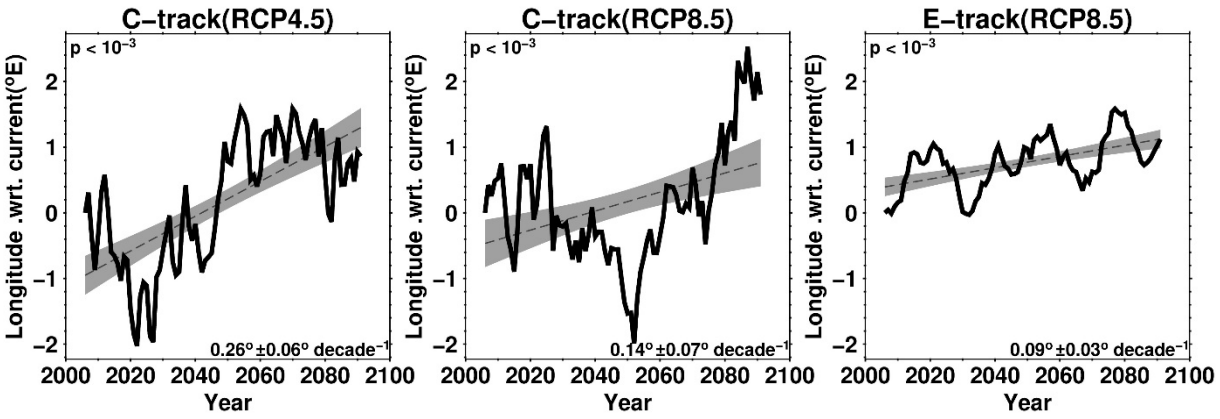

Supplementary Figure 14: MME-averaged longitude time series of the 3 TC track groups, with trends and p-values. 95% confidence trend bounds are shaded.. As in previous work[57], WNP TCs are projected to move eastwards too. Nevertheless, this longitude movement has little impact on PI, as compared to the latitude movement, see Supplementary Figure 15 below.

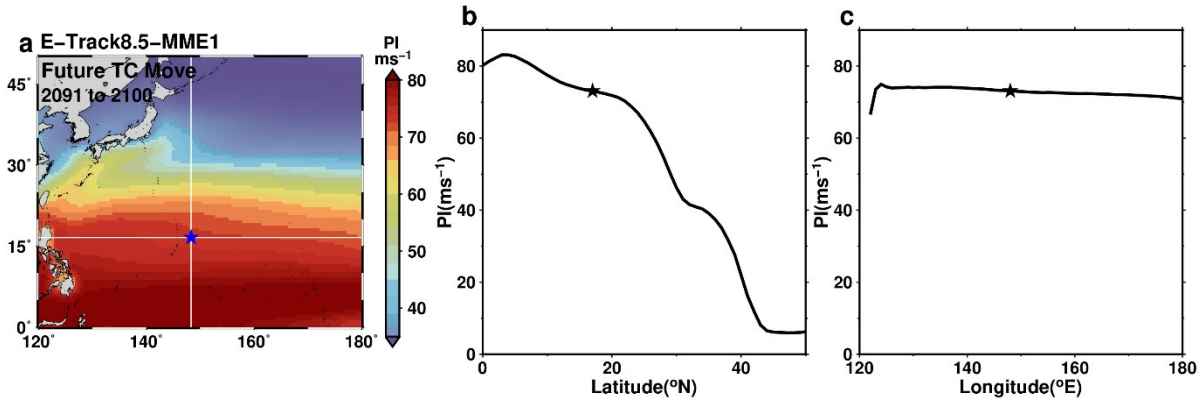

Supplementary Figure 15: (a) WNP PI distribution at 21st century's end (i.e., 2091-2100), with 2 transects across the future TC center (in star), based on E-Track-8.5 MME1. (b) Change in PI along the vertical transect (i.e. w.r.t. latitude change). (c) As in (b), but along the horizontal transect (i.e. w.r.t. longitude change). As in (b, c), the change in PI is mainly in the latitude, and not in the longitude direction.

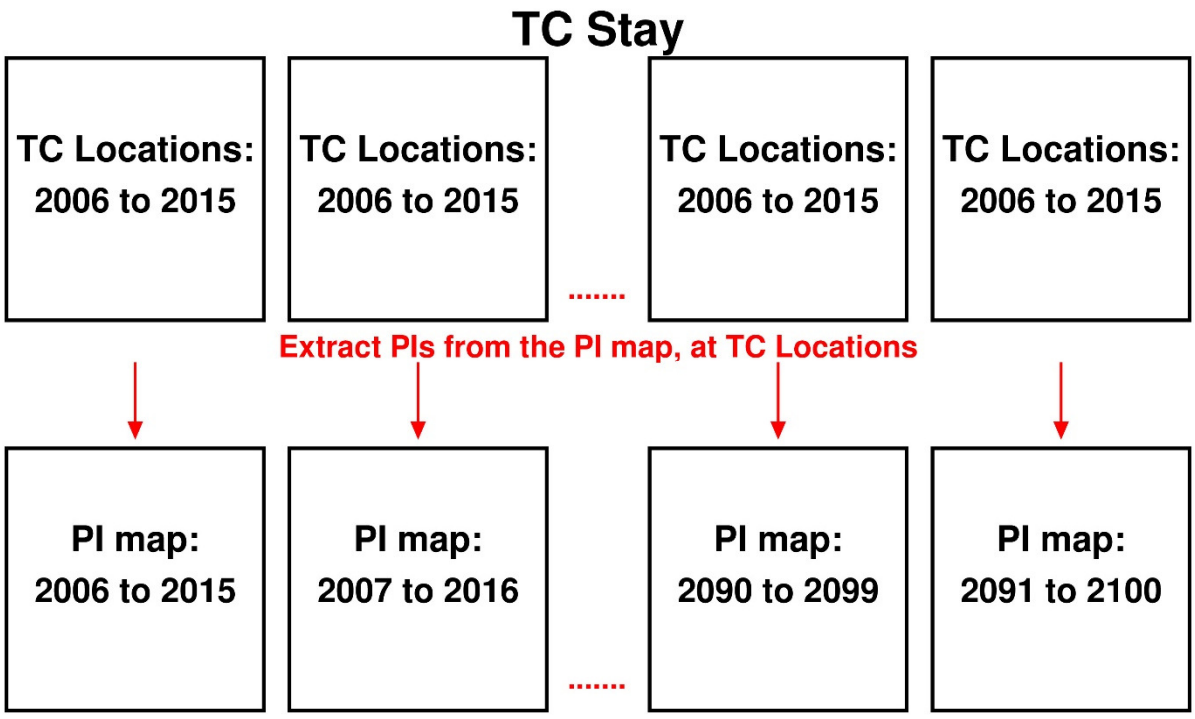

Supplementary Figure 16: For convenience, the extraction of PI samples from the pre-generated 10-year averaged PI maps in the TC_Stay projection.

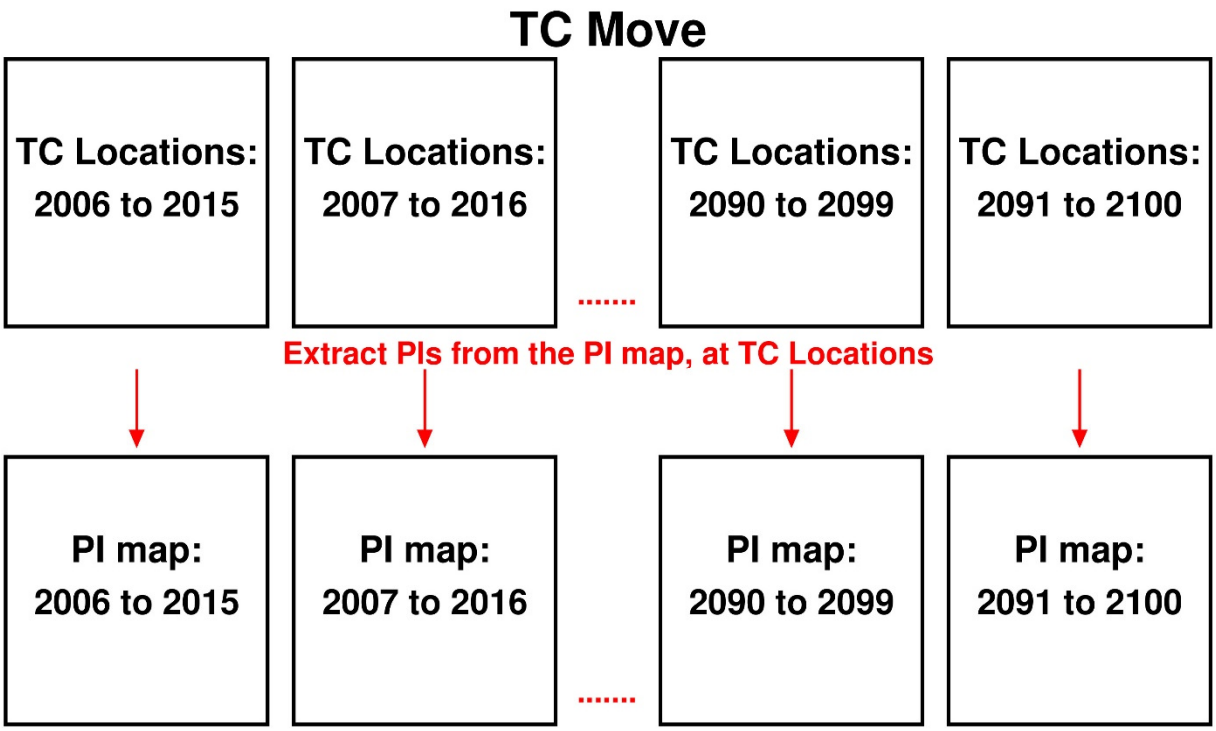

Supplementary Figure 17: For convenience, the extraction of PI samples from the pre-generated 10-year averaged PI maps in the TC_Move projection.

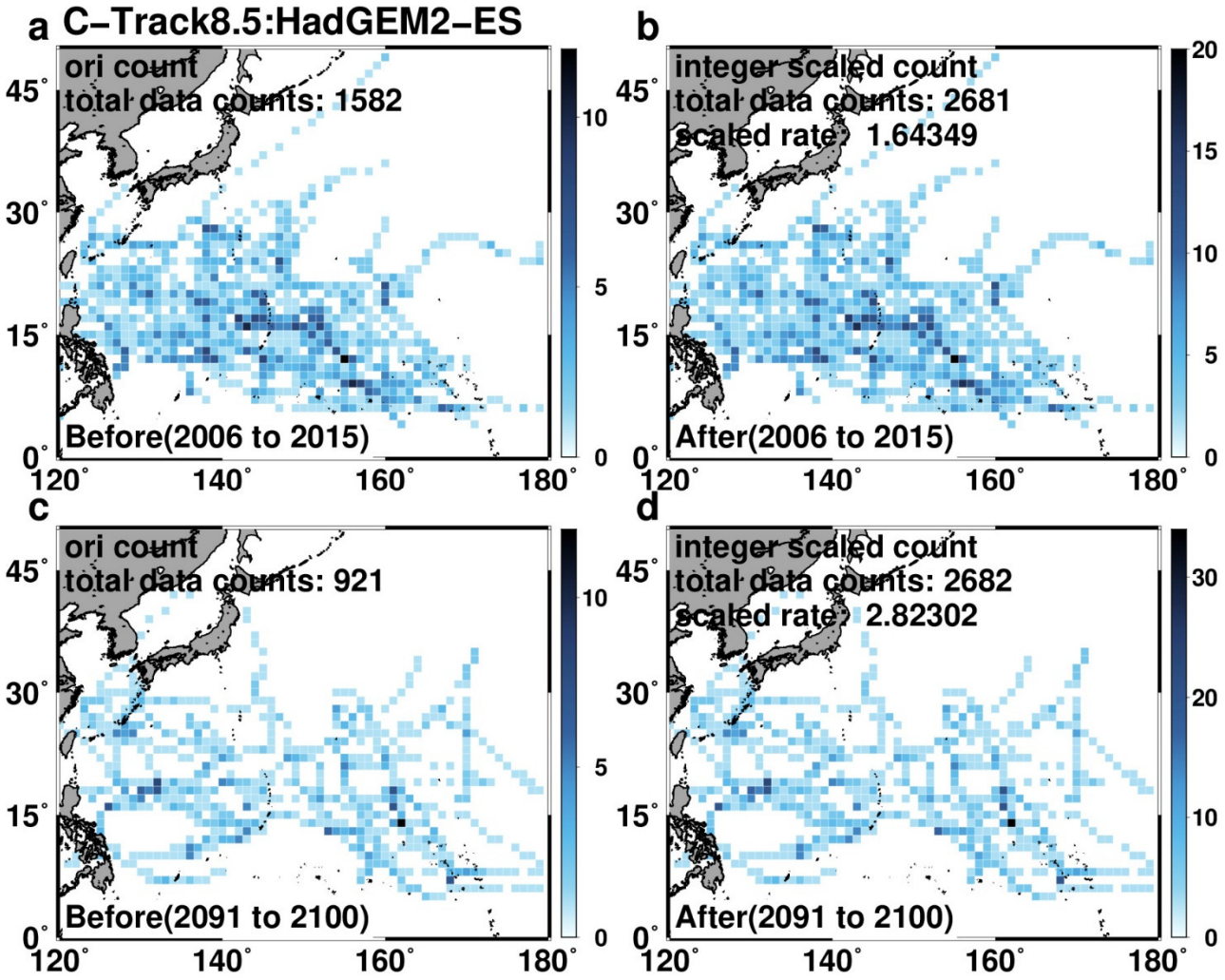

Supplementary Figure 18: TC track point re-scaling for C-Track-8.5, using HadGEMS2-ES model as an example. The top figures depict (a) before, and (b) after rescaling for the current (2006-2015) condition. The bottom figures depict (c) before, and (d) after rescaling for the future condition. As can be seen, the spatial features and characteristics are well-preserved after rescaling.

	C-Track-8.5				E-Track-8.5			
(a) Proportion of Category-5 PI (%)	**MME1**	**MME2**	**MME3**	**MME4**	**MME1**	**MME2**	**MME3**	**MME4**
TC Stay Trend Slope, p, Increase at century's end w.r.t. current	3.09±0.16% decade^{-1}, p<10^{-3} 26.3%	0.91±0.11% decade^{-1}, p<10^{-3} 7.7%	3.22±0.17% decade^{-1}, p< 10^{-3} 27.4%	1.04±0.16% decade^{-1}, p< 10^{-3} 8.9%	2.92±0.13% decade^{-1}, p< 10^{-3} 24.8%	1.52±0.08% decade^{-1}, p< 10^{-3} 12.9%	2.98±0.13% decade^{-1}, p< 10^{-3} 25.3%	1.57±0.08% decade^{-1}, p< 10^{-3} 13.3%
TC Move Trend Slope, p, Increase at century's end w.r.t. current	2.14±0.29% decade^{-1}, p<10^{-3} 18.2%	0.55±0.21% decade^{-1}, p<10^{-3} 4.7%	2.24±0.24% decade^{-1}, p<10^{-3} 19.0%	0.14±0.25% decade^{-1},0.266, 1.2%	1.94±0.11% decade^{-1}, p<10^{-3} 16.5%	0.81±0.08% decade^{-1}, p<10^{-3} 6.9%	2.09±0.11% decade^{-1}, p<10^{-3} 17.8%	0.96±0.08% decade^{-1}, p<10^{-3} 8.1%
Based on the 8 MMEs, the averaged increase at century's end w.r.t. current: TC_Stay (i.e. no poleward migration):18.3%; TC_Move (poleward migration included):11.6%								
	C-Track-8.5				**E-Track-8.5**			
(b) Avg. PI (ms^{-1})	**MME1**	**MME2**	**MME3**	**MME4**	**MME1**	**MME2**	**MME3**	**MME4**
TC Stay Trend Slope, p, Increase at century's end w.r.t. current	0.37±0.02 decade^{-1}, p<10^{-3} 3.1 ms^{-1}	0.36±0.02 decade^{-1}, p< 10^{-3} 3.1 ms^{-1}	0.36±0.02 decade^{-1}, p< 10^{-3} 3.0 ms^{-1}	0.32±0.02 decade^{-1}, p< 10^{-3} 2.7 ms^{-1}	0.29±0.01 decade^{-1}, p< 10^{-3} 2.5 ms^{-1}	0.26±0.01 decade^{-1}, p< 10^{-3} 2.2 ms^{-1}	0.30±0.01 decade^{-1}, p< 10^{-3} 2.5 ms^{-1}	0.27±0.01 decade^{-1}, p< 10^{-3} 2.3 ms^{-1}
TC Move Trend Slope, p, Increase at century's end w.r.t. current	0.12±0.07 decade^{-1}, p<10^{-3} 1.0 ms^{-1}	0.10±0.06 decade^{-1}, 0.001 0.9 ms^{-1}	0.12±0.03 decade^{-1}, p< 10-3 1.0 ms^{-1}	0.01±0.04 decade^{-1}, 0.651 0.1 ms^{-1}	0.11±0.01 decade^{-1}, p< 10^{-3} 0.9 ms^{-1}	0.09±0.01 decade^{-1}, p< 10^{-3} 0.7 ms^{-1}	0.13±0.01 decade^{-1}, p< 10^{-3} 1.1 ms^{-1}	0.12±0.01 decade^{-1}, p< 10^{-3} 1.0 ms^{-1}
Based on the 8 MMEs, the averaged increase at century's end w.r.t. current: TC_Stay (i.e. no poleward migration): 2.7 ms^{-1}; TC_Move (poleward migration included): 0.8 ms^{-1}								

Supplementary Table 1: Summary of the RCP 8.5 Results. Increase at 21st century's end w.r.t current is based on the trend end points. Trend slope and p value are also provided in Table 1 of the main text.

C-Track-4.5				
(a) Proportion of Category-5 PI (%)	**MME1**	**MME2**	**MME3**	**MME4**
TC Stay Trend Slope, p, Increase at century's end wrt. current	1.89±0.12% decade^{-1}, p<10^{-3} 16.0%	0.91±0.09% decade^{-1}, p<10^{-3} 7.7%	2.14±0.14% decade^{-1}, p<10^{-3} 18.2%	1.08±0.17% decade^{-1}, p<10^{-3} 9.2%
TC Move Trend Slope, p, Increase at century's end wrt. current	1.28±0.24% decade^{-1}, p<10^{-3} 10.9%	0.77±0.21% decade^{-1}, p<10^{-3} 6.5%	2.06±0.22% decade^{-1}, p<10^{-3} 17.5%	0.68±0.20% decade^{-1}, p<10^{-3} 5.8%
Based on the 4 MMEs, the averaged increase at century's end w.r.t. current: **TC_Stay (i.e. no poleward migration):12.8%;** **TC_Move (poleward migration included):10.2%**				
C-Track-4.5				
(b) Avg. PI (ms^{-1})	**MME1**	**MME2**	**MME3**	**MME4**
TC Stay Trend Slope, p, Increase at century's end w.r.t. current	0.29±0.01 decade^{-1}, p<10^{-3} 2.4 ms^{-1}	0.27±0.01 decade^{-1}, p<10^{-3} 2.3 ms^{-1}	0.27±0.01 decade^{-1}, p<10^{-3} 2.3 ms^{-1}	0.26±0.01 decade^{-1}, p<10^{-3} 2.2 ms^{-1}
TC Move Trend Slope, p, Increase at century's end w.r.t. current	0.20±0.05 decade^{-1}, p<10^{-3} 1.7 ms^{-1}	0.15±0.06 decade^{-1}, p<10^{-3} 1.3 ms^{-1}	0.25±0.04 decade^{-1}, p<10^{-3} 2.1 ms^{-1}	0.16±0.04 decade^{-1}, p<10^{-3} 1.4 ms^{-1}
Based on the 4 MMEs, the averaged increase at century's end w.r.t. current: **TC_Stay (i.e. no poleward migration): 2.3 ms^{-1};** **TC_Move (poleward migration included): 1.6 ms^{-1}**				

Supplementary Table 2: Summary of the RCP 4.5 Results. Increase at 21st century's end w.r.t current is based on the trend end points. Trend slope and p value are also provided in Table 1 of the main text.

	MME1	MME2	MME3	MME4
Pre-rescaling of TC points **Options: Yes/No**	Yes	Yes	No	No
Sequence in PI map extraction **Options: Option 1/ Option 2**	Option 1	Option 2	Option 1	Option 2

Supplementary Table 3: Summary of the 4 MMEs

(a) C-Track4.5 TC IT Track Points Current (2006-2015)		CanESM2	CSIRO-Mk3-6-0	GFDL-MME	HadGEM2-ES	MRI-CGCM3	Total Counts (100%)
Original Count	Count	877	3,331	4,877	1,710	1,095	11,890
	(%)	7.40%	28.00%	41.00%	14.40%	9.20%	100%
Rescale factor		3.079	0.811	0.554	1.579	2.466	-
After rescale	Count	2,623	2,755	2,855	2,800	2,474	13,507
	(%)	19.40%	20.40%	21.10%	20.70%	18.30%	100%

(b) C-Track4.5 TC IT Track Points Future (2091-2100)		CanESM2	CSIRO-Mk3-6-0	GFDL-MME	HadGEM2-ES	MRI-CGCM3	Total Counts (100%)
Original Count	Count	487	3,941	4,124	1,146	1,190	10,888
	(%)	4.50%	36.20%	37.90%	10.50%	10.90%	100%
Rescale factor		5.544	0.685	0.655	2.356	2.269	-
After rescale	Count	2,789	2,711	2,817	2,624	2,648	13,589
	(%)	20.50%	19.90%	20.70%	19.30%	19.50%	100%

Supplementary Table 4: (a): C-Track-4.5 TC track point counts (and % in the MME) of individual model members, before and after rescaling, for current condition (2006-2015). (b): as in (a), but for future condition (2091-2100). The count reference is 2,700. After rescaling, each of the 5 members (because the 2 GFDL models are first combined into GFDL-MME, see Methods) have counts ~ 2,700 and contributes similarly (i.e., ~ 20%) towards the MME.

(a) C-Track8.5 TC IT Track Points Current (2006-2015)		CSIRO-Mk3-6-0	GFDL-MME	HadGEM2-ES	IPSL-CM5A-LR	MRI-CGCM3	Total Counts (100%)
Original Count	**Count**	4,158	4,523	1,582	960	1,187	12,410
	(%)	33.5%	36.4%	12.7%	7.7%	9.6%	100%
Rescale factor		0.625	0.575	1.643	2.708	2.19	-
After rescale	**Count**	2,733	2,727	2,681	2,628	2,461	13,230
	(%)	20.7%	20.6%	20.3%	19.9%	18.6%	100%

(b) C-Track8.5 TC IT Track Points Future (2091-2100)		CSIRO-Mk3-6-0	GFDL-MME	HadGEM2-ES	IPSL-CM5A-LR	MRI-CGCM3	Total Counts (100%)
Original Count	**Count**	4,236	4,257	921	649	1,362	11,425
	(%)	37.1%	37.3%	8.1%	5.7%	11.9%	100%
Rescale factor		0.614	0.611	2.823	4.006	1.909	-
After rescale	**Count**	2,652	2,675	2,682	2,588	2,688	13,285
	(%)	20.0%	20.1%	20.2%	19.5%	20.2%	100%

Supplementary Table 5: (a): C-Track-8.5 TC track point counts (and % in the MME) of individual model members, before and after rescaling, for current condition (2006-2015). (b): as in (a), but for future condition (2091-2100). The count reference is 2,600. After rescaling, each of the 5 members (because the 2 GFDL models are first combined into GFDL-MME, see Methods) have counts ~ 2,600 and contributes similarly (i.e., ~ 20%) towards the MME.

(a) E-Track 8.5 TC IT Track Points Current (2006-2015)		GFDL-CM3	HadGEM2-ES	IPSL-CM5A-LR	MIROC5	MPI-ESM-MR	MRI-CGCM3	SP-CCSM4	Total Counts (100%)
Orig. Count	Count	48,183	54,547	58,904	36,210	52,385	53,025	54,575	357,829
	(%)	13.5%	15.2%	16.5%	10.1%	14.6%	14.8%	15.3%	100%
Rescale factor		1.038	0.917	0.849	1.381	0.954	0.943	0.916	-
After rescale	Count	49,618	49,967	49,912	49,887	49,925	49,816	49,768	348,893
	(%)	14.2%	14.3%	14.3%	14.3%	14.3%	14.3%	14.3%	100%

(b) E-Track 8.5 TC IT Track Points Future (2091-2100)		GFDL-CM3	HadGEM2-ES	IPSL-CM5A-LR	MIROC5	MPI-ESM-MR	MRI-CGCM3	SP-CCSM4	Total Counts (100%)
Orig. Count	Count	50,293	49,495	60,249	30,633	59,283	54,182	52,484	356,619
	(%)	14.1%	13.9%	16.9%	8.6%	16.6%	15.2%	14.7%	100%
Rescale factor		0.994	1.01	0.83	1.632	0.843	0.923	0.953	-
After rescale	Count	50,061	49,537	49,684	49,880	49,859	49,800	49,891	348,712
	(%)	14.4%	14.2%	14.2%	14.3%	14.3%	14.3%	14.3%	100%

Supplementary Table 6: (a): E-Track-8.5 TC track point counts (and % in the MME) of individual model members, before and after rescaling, for current condition (2006-2015). (b): as in (a), but for future condition (2091-2100). The count reference is 50,000. After rescaling, each of the 7 members contributes similarly (i.e., ~ 14.3%) towards MME.

Supplementary Note 1

Poleward migration and ocean subsurface factor

As in the Discussion Section, though it is outside the main scope of this research, we still conduct some preliminary assessment on the possible effect from ocean subsurface change associated with poleward migration. In the original PI formulation, the inputs are sea surface temperature (SST), atmospheric temperature profile, atmospheric humidity profile, and sea level pressure[41]. Contribution from ocean subsurface stratification (i.e., thermal profile) is not included. In 2013, a revised index, called Ocean Coupling Potential Intensity (OCPI) [52,53] was developed to include the ocean subsurface contribution, and is used here to aid the diagnosis. Two E-Track-8.5 models, SP-CCSM4 and HADGEMS2-ES, are tested. The results are consistent and the SP-CCSM4 result is discussed here. The HADGEMS2-ES results are in Supplementary Figure 10. We first examine the initial ocean subsurface thermal profiles. For the 'with poleward migration' situation, the ocean profile used is the averaged profile along the intensification track points in the TC_Move scenario. For the 'without poleward migration' situation, the ocean profile is the averaged profile along the intensification track points in the TC_Stay scenario. Also, the profile is the average in the TC Season (June-November), from the original monthly field. Vertically, the input profile is from 0-1000m depth. The original ocean fields of the 2 models are from the CMIP5 web (https://esgf-node.llnl.gov/search/cmip5/), under the RCP 8.5 scenario. When poleward migration is included (i.e., taking ocean profiles along the TC_Move tracks), ocean stratification change between current and future is sharper than in the 'no poleward migration' case (i.e. profiles taken along the TC_Stay tracks). As in Panels a and b below, the difference between the warming w.r.t. current at 100m and SST is -0.26˚C (i.e., 2.57 ˚C -2.83 ˚C) in (a), but is -0.48 ˚C (i.e., 2.28 ˚C -2.76 ˚C) in (b). Using these profiles as input, we use the 3D Price-Weller-Pinkel (3DPWP, Price et al. 1994[50]) ocean model to estimate the TC-induced ocean cooling effect (aka cooling effect)[46,51]. As in Panel c below, the averaged cooling effect is -0.11˚C, -0.17 ˚C, and -0.18˚C for current, TC_Stay future scenario, and TC_Move future scenario, respectively. OCPI has 5 inputs, pre-TC SST, atmospheric temperature profile, atmospheric humidity profile, sea level

pressure, and the cooling effect[52]. As in Panel c, the change in OCPI w.r.t. current for the TC_Stay future scenario is 1.74 ms^{-1} and 0.79 ms^{-1} for the TC_Move future scenario. Because the difference between TC_Move and TC_Stay is poleward migration's impact, this impact is -0.95 ms^{-1}. Remember OCPI has 5 inputs, the 0.95 ms^{-1} difference is from the contributions of 5 inputs' poleward shift. As for the original PI, the difference between TC_Stay and TC_Move is -0.86 ms^{-1}, this is contributed by the poleward change from the 4 inputs. Because the inputs for OCPI and PI are identical except the cooling effect, the -0.09 ms^{-1} difference between -0.95 and -0.86 ms^{-1} is the contribution from the cooling effect (i.e., ocean subsurface stratification contribution). This accounts for ~ 9% in the total change from all 5 inputs (-0.09/-0.95). In other words, the other 4 inputs (i.e. the ones used in the PI) account for ~91%. Thus ocean subsurface factor does contribute to increase the negative effect, though does not appear to be too large. The original PI should have captured the primary contributions.

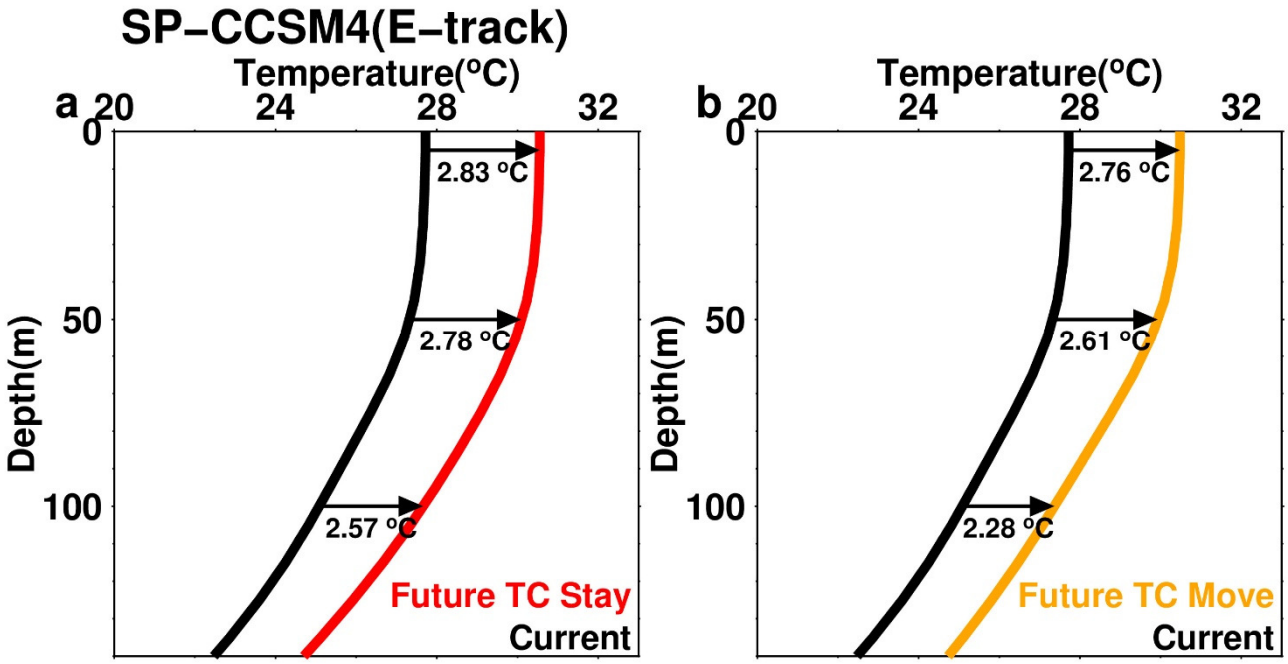

(c) E-Track-8.5/SP-CCSM4	Current	Future TC Stay	Future TC Move
Pre-TC SST (˚C)	27.72	30.55	30.48
SST cooling (˚C)	-0.11	-0.17	-0.18
PI change w.r.t current (ms^{-1})	-	2.51	1.65
OCPI change w.r.t current (ms^{-1})	-	1.74	0.79

- PI: Difference between Future TC-Move and Future TC Stay is -0.86 ms^{-1} (i.e., 1.65 - 2.51). This difference is contributed by the 4 PI inputs.
- OCPI: Difference between Future TC-Move and Future TC Stay is -0.95 ms^{-1} (i.e., 0.79-1.74). This difference is contributed by the 5 OCPI inputs.
- The difference between -0.86 ms^{-1} and -0.95 ms^{-1}, i.e. -0.09 ms^{-1} is the contribution from ocean cooling (stratification) input. Thus ocean stratification contributes to ~ 9% in the total contribution from all 5 inputs (-0.09/-0.95).

Panel: (a) Initial ocean thermal profiles for Current (black) and TC_Stay future scenario (red).

(b) Initial ocean thermal profile for Current (black) and TC_Move future scenario (yellow).

(c) Results of the ocean cooling effect, PI, and OCPI (Ocean Coupling Potential Intensity).

Supplementary Note 2

PI distribution

Complementing Fig. 5 in the main text, we illustrate the PI probability distribution histograms (Figs. abc below). In comparison with the current climate distribution (Fig. a), there is a shift towards the higher PI values in the TC_Stay future scenario (Fig. b). For the TC_Move future scenario, increases in both high and low values of the distribution are present (Fig. c). 'Record breaking PI occurrences' (i.e., PI values exceeding the current maximum PI value) are found in both future scenarios (yellow bars in Figs. b and c), though the magnitude for the TC_Move scenario is smaller.

As in the main text, due to global warming's positive impact, the shift towards the high-values and occurrence of record-breaking PIs are expected in the TC_Stay future scenario (Fig. b and Fig. 5b in the main text). For the TC_Move future scenario, because global warming's positive impact and poleward migration's negative impact are both at work (Fig. c and Fig. 5c in the main text), increase in both ends of the spectrum is seen. The increase in the low PI samples is because there are more samples from the higher latitudes. The reason for increase in the high PI samples (including record breaking PIs) being also present in the TC_Move PI projection is that although poleward migration occurs, it is a gradual process. In terms of absolute latitude (e.g., ≤ 18˚N), there are considerable TC locations still remain at south (Fig. f and Fig. 5c in the main text), and their PI values will still increase with global warming in a region that already has high PI values.

Finally, comparing Figs. a and b, the increase in the average PI value for future TC_Stay w.r.t current is ~2.51 ms^{-1} (73.32-70.81 ms^{-1}). This amount is similar to the values reported in the existing literature which does not consider poleward migration's impact[13], and can also be seen from the red curve in Fig. 4c of the main text. On the other hand, for TC_Move the increase in the average PI w.r.t current is much smaller, i.e., only ~ 0.65ms^{-1} (71.46-70.81ms^{-1}, cf. Figs. a and c). This is because the increase in both high and low-ends of the spectrum compensate each other (see further information in the figure

caption below). This distribution reminds us that even if the averaged PI increase is small, there can still be considerable increase in the high-end (e.g., Category-5) PIs. Thus, when viewing the gentle increase in the black curve of Fig. 4c in the main text, it is important to bear in mind these distribution changes.

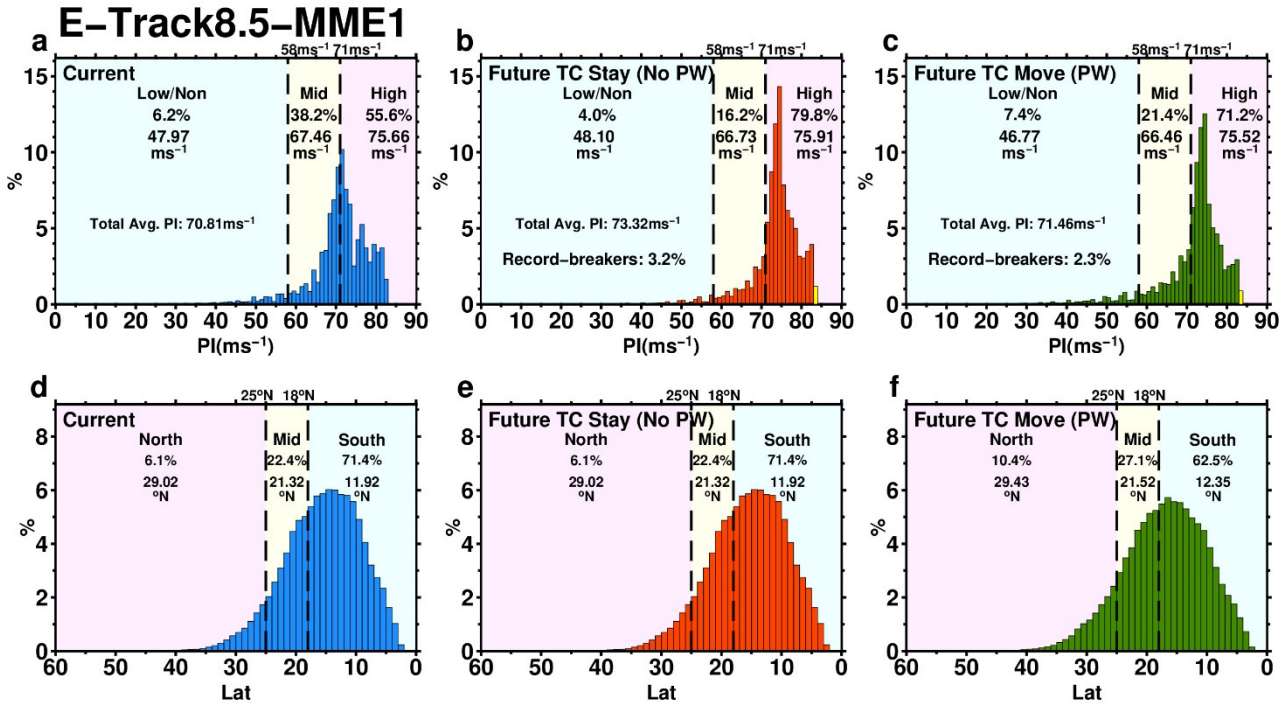

Complementing Fig. 5 in the main text, PI probability distribution histograms of E-Track-8.5 MME1. Top (a, b, c): (a) Current, (b) TC_Stay future scenario, and (c) TC_Move future scenario. For convenience, PI distribution is separated into 3 sub-groups: high-intensifiers ($\geqq$ 71 ms^{-1}, or Category-5 PI), mid-intensifiers (58 to < 71 ms^{-1}, or Category-4 PI), and low/non intensifiers (<58 ms^{-1}, Category-3 and below). Record breaker is depicted in yellow. Comparing (a) and (c), it can be seen that the averaged PI values are similar, i.e., 70.81 .vs. 71.46 ms^{-1}. This is because the high and low-end increases compensate each other. The averaged values of all 3 subgroups in (c) are also lower than in (a). Bottom (d, e, f): Latitude probability distribution, with x-axis increases from right to left. Latitudes are also separated into 3 sub-group: South: 0-18°N; Mid:> 18°N to $\leqq$ 25°N; North: > 25°N-90°N.